

Three-Dimensional Distributions of Type II Cepheids and Anomalous Cepheids in the Magellanic Clouds.**Do these Stars Belong to the Old, Young or Intermediate-Age Population?**

P. Iwanek¹, I. Soszyński¹, D. Skowron¹, J. Skowron¹,
P. Mróz¹, S. Kozłowski¹, A. Udalski¹, M. K. Szymański¹,
P. Pietrukowicz¹, R. Poleski^{2,1} and A. Jacyszyn-Dobrzeńska¹

¹Warsaw University Observatory, Al. Ujazdowskie 4, 00-478 Warsaw, Poland
e-mail: piwanek@astrouw.edu.pl

²Department of Astronomy, Ohio State University, 140 W. 18th Ave., Columbus, OH
43210, USA

Received September 9, 2018

ABSTRACT

The nature of type II Cepheids and anomalous Cepheids is still not well known and their evolutionary channels leave many unanswered questions. We use complete collection of classical pulsating stars in the Magellanic Clouds discovered by the OGLE project, to compare their spatial distributions, which are one of the characteristic features directly related to the star formation history. In this analysis we use 9649 classical Cepheids, 262 anomalous Cepheids, 338 type II Cepheids and 46 443 RR Lyr stars from both Magellanic Clouds. We compute three-dimensional Kolmogorov-Smirnov tests for every possible pair of type II and anomalous Cepheids with classical Cepheids, and RR Lyr stars. We confirm that BL Her stars are as old as RR Lyr variable stars – their spatial distributions are similar, and they create a vast halo around both galaxies. We discover that spatial distribution of W Vir stars has attributes characteristic for both young and old stellar populations. Hence, it seems that these similarities are related to the concentration of these stars in the center of the Large Magellanic Cloud, and the lack of a vast halo. This leads to the conclusion that W Vir variables could be a mixture of old and intermediate-age stars. Our analysis of the three-dimensional distributions of anomalous Cepheids shows that they differ significantly from classical Cepheids. Statistical tests of anomalous Cepheids distributions with RR Lyr distributions do not give unambiguous results. We consider that these two distributions can be similar through the vast halos they create. This similarity would confirm anomalous Cepheids evolution scenario that assumes coalescence of a binary system.

Key words: *Stars: variables: Cepheids – Stars: variables: RR Lyrae – Magellanic Clouds*

1. Introduction

Many years of research on the pulsating stars, including famous discovery of the period–luminosity (PL) relation (Leavitt and Pickering 1912), made classical

pulsators the primary distance indicators in the nearby Universe. Subsequent discoveries of pulsating stars led to the distance scale revision done by Baade (1952), who noted that there are two different groups of Cepheids which follow different PL relations. Hence, the Cepheids were divided into Population I (called classical Cepheids – DCEPs) and Population II (called type II Cepheids – T2CEPs). Nowadays, T2CEPs are divided into three subgroups depending on their pulsation period P : BL Her ($P < 4$ d), W Vir ($4 \text{ d} \leq P < 20$ d) and RV Tau ($P > 20$ d). The boundaries in the pulsation periods for these stars are not strict, and these groups partly overlap. Additionally, Soszyński *et al.* (2008) distinguished a fourth subgroup of T2CEPs, named peculiar W Vir stars.

After over sixty years of study of T2CEPs their origin and evolution channels are still not clear. The first evolution scenarios of these stars were proposed by Gingold (1976, 1985). The most up-to-date review of the T2CEPs properties has been done by Welch (2012). It is believed that these objects are low-mass stars belonging to the halo and old disk stellar populations. BL Her stars evolve from blue horizontal giant branch to asymptotic giant branch. During evolution these stars become brighter and their radii increase, which is associated with helium burning in the cores. BL Her variables pass through the instability strip at luminosities, which correspond to the pulsation periods shorter than 4 d. RV Tau variables are post-asymptotic giant branch stars just before the outer envelope expulsion, which is supposed to form a planetary nebula, and a core that becomes a white dwarf. These stars pass through the high-luminosity extension of the Cepheid instability strip which corresponds to pulsation periods longer than 20 d. The origin of W Vir stars is the most incomprehensible. It is believed that these variables are asymptotic giant branch stars that have exhausted helium in their cores, and they start burning helium in the shell. The helium shell burning causes a gradual reduction of the energy supply from the hydrogen shell, which in turn leads to the stoppage of energy production in the hydrogen shell. The hydrogen shell burning may re-switch due to heating arising from contraction. Switching on and off of the shells burning may cause blue loops in the instability strip. The loops are expected only in stars with small enough external envelope, and they could be recurring (Cassisi and Salaris 2013), but modern calculations are not able to reproduce this scenario. So far, there are no evolutionary channels that would explain the origin of W Vir variable stars (Groenewegen and Jurkovic 2017a).

Soszyński *et al.* (2008) found evidences that peculiar W Vir stars have companions. The evolution in a binary system provides conditions conducive to the occurrence of pulsations. Up-to-date, 50% of known peculiar W Vir stars from the Magellanic Clouds have clear signs of binarity in the light curves.

In Fig. 1 we present distributions of T2CEPs in the sky. Positions of BL Her and W Vir stars show a large scatter in both Magellanic Clouds. RV Tau stars seem to be more concentrated around the centers of the Large Magellanic Cloud (LMC)

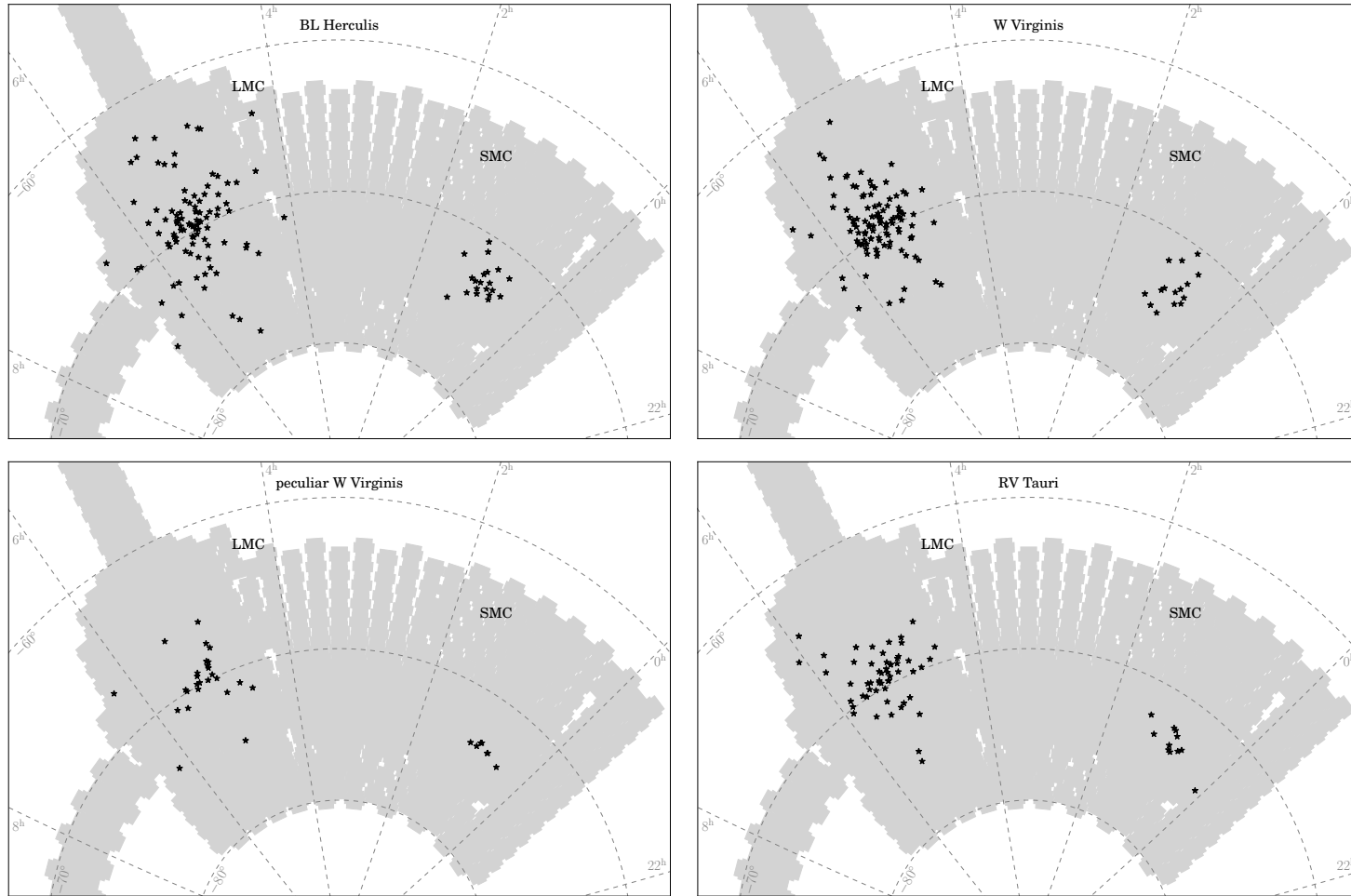


Fig. 1. Distributions of T2CEPs in the sky. The gray area presents the OGLE-IV footprint.

and Small Magellanic Cloud (SMC). Peculiar W Vir stars have slightly different positions in the sky than other T2CEPs – they are mostly clumped around the bar of the LMC and they are located in the center of the SMC. In addition, T2CEPs are found in globular clusters in the LMC, with exception of peculiar W Vir stars (Matsunaga *et al.* 2009). All these properties suggest that BL Her, W Vir and RV Tau variables very likely belong to the old population, while peculiar W Vir stars may be younger.

Observations of dwarf galaxies in the 50s and 60s of the 20th century showed the existence of another group of pulsating stars, which brightness variations did not match any of the known groups (Thackeray 1950). For this reason this group has been called anomalous Cepheids – ACEPs (Zinn and Searle 1976). The existence of this group of pulsating stars can be explained in two ways: by evolution of single intermediate-mass, metal-deficient star, which burns helium in the core, or as the effect of coalescence of two old, low-mass stars which evolved in the binary system. Fiorentino and Monelli (2012) found that ACEPs distribution is different than DCEPs or RR Lyr stars distributions. They also suggested that observations of the LMC outskirts could be helpful to solve the problem of ACEPs origin.

In Fig. 2, we present sky distribution of ACEPs in the LMC, and SMC. It is clearly seen that these type of pulsating stars create a vast halo around the Clouds. Moreover, there are a few objects in the area between the Magellanic Clouds (called Magellanic Bridge). Therefore, the distribution suggests that these stars belong to the population as old as RR Lyr variables or even older, or they could reside in the Galactic foreground.

In this paper we use our complete collection of pulsating stars discovered in the OGLE-IV data to compare three-dimensional distributions of pulsators in the Magellanic Clouds. Our knowledge about evolutionary status of DCEPs and RR Lyr stars is more complete compared to what we know about T2CEPs or ACEPs. We

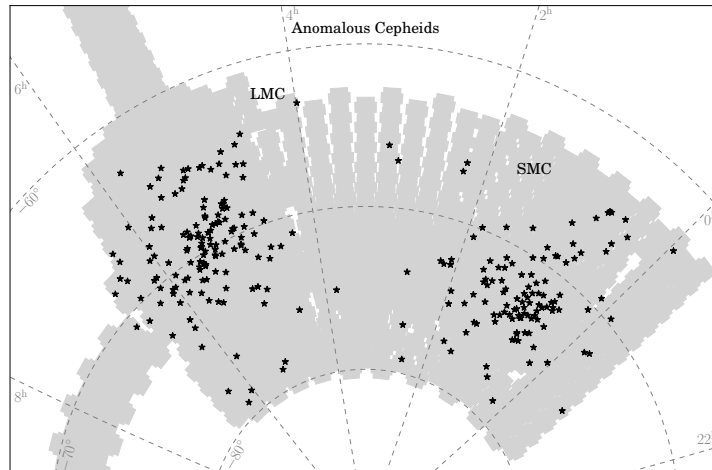


Fig. 2. Distribution of ACEPs in the sky. The gray area presents the OGLE-IV footprint.

believe that the comparison of the distributions of T2CEPs and ACEPs with other classical pulsators distributions could shed light on the history and the future of these stars. The spatial distribution of T2CEPs and ACEPs may be a key to understanding their origin.

The paper is organized as follows. In Section 2, we discuss pulsating star samples selection, which we use in our analysis. The distance determination method used in this paper and transformation of coordinates to the Cartesian space and Hammer equal-area projection are presented in Section 3. Section 4 contains a detailed discussion of the method of performing three-dimensional Kolmogorov-Smirnov statistical test. In Section 5, we discuss results of our analysis with probable evolution scenarios for each group of T2CEPs and ACEPs. We compare the decision-making methods in Section 6. Finally, in Section 7 we summarize our results.

2. Sample Selection

The photometric data obtained by the Optical Gravitational Lensing Experiment (OGLE) over 25 years of its activity has allowed to increase the number of known classical pulsating stars by a large factor. At this moment our collection contains 9649 DCEPs, 262 ACEPs, 338 T2CEPs and 46 443 RR Lyr stars in the Magellanic System (Soszyński *et al.* 2017), which is the most complete and the largest list of classical pulsators in these galaxies. The entire collection is available on-line *via* the OGLE FTP site:

ftp://ftp.astrouw.edu.pl/ogle/ogle4/OCVS/

Details about the OGLE instrumentation, data reductions, calibrations, sky coverage and observing cadence can be found in Udalski *et al.* (2015).

In our study, we use stars with a single radial mode excited. It is worth mentioning, however, that a recent research showed presence of additional low-amplitude periodicities in stars classified as single-mode pulsators. Netzel *et al.* (2015) showed that 27% of the first overtone RR Lyr stars (RRc) have additional periodicities, which can be interpreted as caused by non-radial modes (Dziembowski *et al.* 2016). Moskalik *et al.* (2015) analyzed observations of RRc stars from the Kepler satellite and they found low-amplitude non-radial modes excited in every considered star. The same phenomenon was observed in the first overtone DCEPs (Soszyński *et al.* 2015c, Smolec and Śniegowska 2016, Süveges and Anderson 2018) and fundamental-mode pulsators (*e.g.*, Smolec *et al.* 2016, Prudil *et al.* 2017). The additional periodicities usually have low amplitudes and so do not influence the inferred distances.

Another noteworthy aspect is an amplitude and phase modulations present in some single-mode stars. The most pronounced effect of this type with a high incidence rate is the Blazhko effect. This phenomenon is noticeable in the fundamental-

mode RR Lyr stars (RRab – Prudil and Skarka 2017), and recently Netzel *et al.* (2018) showed that 5.6% of RRC stars from the OGLE sample show Blazhko modulations.

The OGLE collection of DCEPs in the Magellanic Clouds consist of 9649 stars (Soszyński *et al.* 2015b, 2017). For our analysis we use DCEPs which pulsate solely in the fundamental mode (F-mode – 5229 objects in total) or solely in the first overtone (1O – 3568 objects in total) as the most numerous samples. 2476 of the F-mode and 1775 of the 1O DCEPs are located in the LMC, whereas 2753 F-mode and 1793 1O DCEPs are located in the SMC.

The OGLE sample of pulsating stars consists of 46 443 RR Lyr variables (Soszyński *et al.* 2016, 2017). We choose RR Lyr stars which pulsate solely in the fundamental mode (RRab – 33 297 objects) or solely in the first overtone (RRC – 10 464 objects). 28 192 RRab stars are located in the LMC and the rest of the sample (5105 objects) are located in the SMC. In the case of the RRC stars we have 9663 objects in the LMC and 801 stars in the SMC. Some of these stars may belong to the Milky Way halo. In the LMC center blending and crowding effects may influence the three-dimensional distribution of RR Lyr stars (Jacyszyn-Dobrzaniecka *et al.* 2017). To partially eliminate blended RRab variables, we reject all objects for which peak-to-peak *I*-band amplitudes $A_I < -5 \cdot \log(P) - 1$, where P is the pulsating period in the F-mode (the Bailey diagram, see Fig. 1 in Jacyszyn-Dobrzaniecka *et al.* 2017). After this rejection we are left with 26 681 RRab stars in the LMC and 5018 objects in the SMC.

Our collection of T2CEPs in the Magellanic Clouds contains 338 stars in total (285 stars in the LMC and 53 objects in the SMC, Soszyński *et al.* 2017, 2018). We subdivide T2CEPs by the pulsation period. In the entire collection, we have 98 BL Her stars in the LMC, and 20 stars in the SMC, 106 W Vir objects in the LMC, and 15 objects in the SMC, and 55 RV Tau stars in the LMC, and 11 such stars in the SMC. The least numerous group is peculiar W Vir stars. Our sample contains 26 these objects in the LMC, and 7 objects in the SMC.

To date, the OGLE project has found 262 ACEPs in the Magellanic System (Soszyński *et al.* 2015a, 2017). As before, we choose for our analysis stars which pulsate solely in the fundamental mode or solely in the first overtone. 102 F-mode pulsators are located in the LMC, and 78 are located in the SMC. In the case of the 1O ACEPs, we have 41 objects in the LMC, and the same number in the SMC.

In Table 1, we present final number of objects used in this analysis (N_{fin}) after all selection cuts and after σ -clipping procedure (described in detail in Section 3).

3. Determination of the Distances to the Pulsating Stars

All of the pulsating stars analyzed in this paper, with the exception of peculiar W Vir stars, follow PL relations, which allow us to calculate their distances. However, PL relation for RV Tau stars are uncertain due to the large internal scatter

Table 1

PL relations for each type of pulsating stars in the Magellanic Clouds analyzed in this paper

Galaxy	Type of stars	a	b	N_{fin}
LMC	F-mode Cepheids	-3.319 ± 0.008	15.892 ± 0.005	2203
	1O Cepheids	-3.440 ± 0.008	15.398 ± 0.003	1594
	RRab	-2.975 ± 0.016	17.167 ± 0.004	23265
	RRc	-3.109 ± 0.026	16.682 ± 0.013	8376
	BL Her	-2.683 ± 0.091	17.356 ± 0.024	79
	W Vir	-2.536 ± 0.060	17.378 ± 0.062	94
	F-mode ACEPs	-2.957 ± 0.118	16.591 ± 0.018	94
	1O ACEPs	-3.298 ± 0.200	16.041 ± 0.041	39
SMC	F-mode Cepheids	-3.448 ± 0.011	16.496 ± 0.005	2565
	1O Cepheids	-3.570 ± 0.020	15.969 ± 0.005	1682
	RRab	-3.321 ± 0.063	17.440 ± 0.014	4378
	RRc	-3.262 ± 0.139	16.986 ± 0.065	639
	BL Her	-2.753 ± 0.403	17.630 ± 0.104	20
	W Vir	-2.688 ± 0.156	17.976 ± 0.164	15
	F-mode ACEPs	-2.887 ± 0.140	16.950 ± 0.021	72
	1O ACEPs	-3.686 ± 0.275	16.545 ± 0.049	39

along relation, and small number of objects in the Magellanic Clouds. This makes the measured distances to these stars unreliable. For this reason we decide not to carry out the three-dimensional analysis of this T2CEPs subgroup.

We fit PL relations, separately for every group of pulsating stars listed in Table 1. We use the reddening-independent Wesenheit index (Madore 1976) defined as follows:

$$W_I = I - 1.55 \cdot (V - I). \quad (1)$$

The 1.55 coefficient is calculated from the standard interstellar extinction curve dependence of the I -band extinction on $E(V - I)$ reddening (Schlegel *et al.* 1998). Jacyszyn-Dobrzniecka *et al.* (2016) examined Wesenheit index with coefficient 1.44 (Udalski 2003). They found that for these two coefficients there is no significant difference in geometry of the Magellanic System.

In this study, we marginalize the impact of metallicity ($[\text{Fe}/\text{H}]$) on the PL relations. For DCEPs this is a commonly used approach as many studies have shown that the impact of metallicity on the PL relations is negligible (Caputo *et al.* 2000, Romaniello *et al.* 2008, Bono *et al.* 2008, Freedman and Madore 2011, Wielgórski *et al.* 2017, Gieren *et al.* 2018). For RR Lyr stars, the metallicity influences the morphology of the horizontal branch, and so the optical PL relations (*i.e.*, Catelan *et al.* 2004, Braga *et al.* 2015). The dependence of light curve parameters on metallicity is significant and has been long studied (see Skowron *et al.* 2016 and references therein). We compared mean distances to the LMC and SMC calculated using both approaches – taking into account (Jacyszyn-Dobrzniecka 2017) and ignoring the

impact of the metallicity (from this work) on the PL relations. We found that the difference in the distance to the LMC is at the level of about 1%, while for the SMC it is at level of about 3%. Therefore, we think that distance determination without taking into account the metallicity is sufficient for this work. It is noteworthy, however, that while this approach is acceptable for statistical analysis of large sample of classical pulsators, it may cause incorrect distances to individual stars, mostly to extremely metal-rich or extremely metal-poor objects.

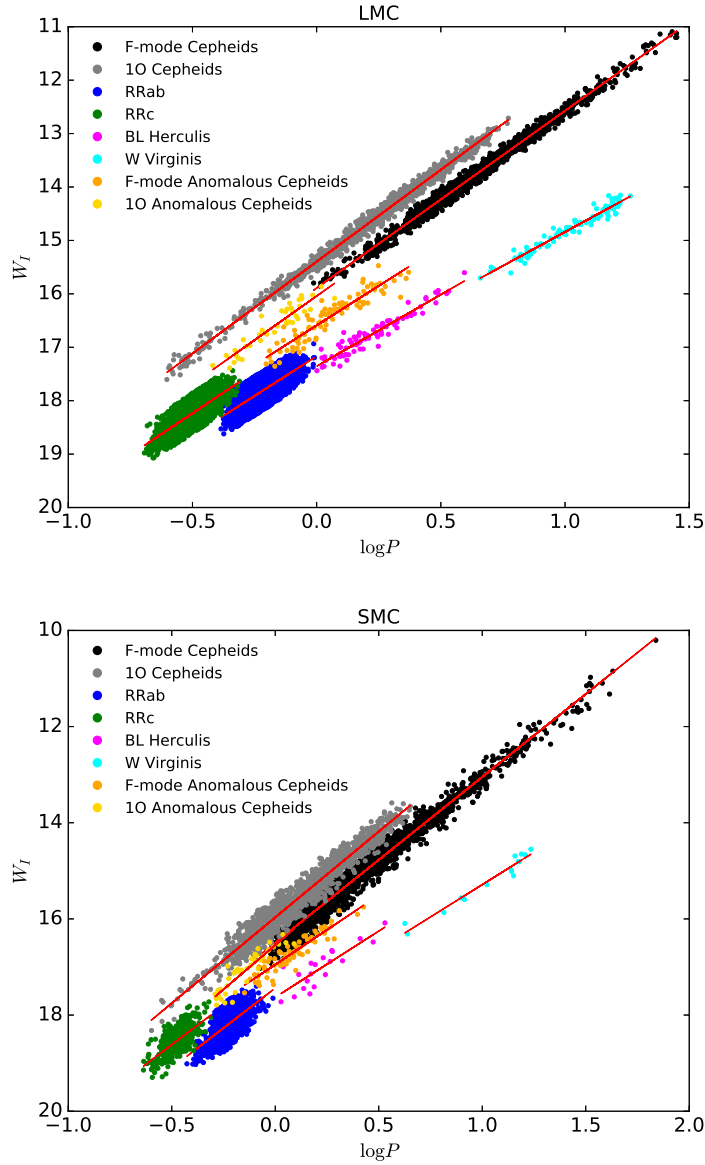


Fig. 3. PL diagrams for DCEPs, ACEPs T2CEPs, and RR Lyr variables in the Magellanic Clouds. We present PL relations after all selection cuts and σ -clipping procedure.

Stars that do not have measurements in both I - and V -band are rejected from further analysis. Using the ordinary least square method and σ -clipping procedure for each dataset we iteratively fit a linear function in the form:

$$W_I = a \cdot \log(P) + b. \quad (2)$$

In each iteration, we reject points deviating more than 3σ from the predicted W_I until none were rejected. The majority of the rejected outliers are due to blending and crowding effects. The PL diagrams for all analyzed groups of pulsating stars in the Magellanic Clouds are shown in Fig. 3. In Table 1, we present the fitted PL relations (a and b coefficients with appropriate uncertainty) for each dataset with the remaining number of objects (N_{fin}) after all iterations.

We are aware that σ -clipping method is not the most appropriate for studies of three-dimensional distributions as it was shown by Deb *et al.* (2018) and Nikolaev *et al.* (2004), that the error distribution is not normal for Wesenheit index at a given period (*e.g.*, due to geometry of the Clouds). The application of this method would cause some objects that are genuinely located closer or farther than the entire LMC/SMC sample to be rejected as outliers. However, other studies (*i.e.*, Jacyszyn-Dobrzeniecka *et al.* 2016, 2017, Inno *et al.* 2016) proven that this method is robust enough for studying three-dimensional samples. Therefore, we decided to use it again in this study.

Comparing PL relations for DCEPs and RR Lyr stars derived in this work with that found by Jacyszyn-Dobrzeniecka *et al.* (2016, 2017), we can see that a and b coefficients marginally differ. This is mostly due to using slightly different samples in these studies and this paper. Here we use the latest published version of the OGLE collection of pulsating stars (Soszyński *et al.* 2017), which was updated with a number of new objects as compared to the samples used by Jacyszyn-Dobrzeniecka *et al.* (2016, 2017). Additionally, the differences in PL relations for DCEPs may be caused by the fact that Jacyszyn-Dobrzeniecka *et al.* (2016) used multimode as well as single-mode pulsators to determine PL relations, while in this study we only use single-mode stars.

The most up-to-date PL relations for T2CEPs and ACEPs were published by Groenewegen and Jurkovic (2017b, see Table 1). These relations are slightly different than ours (see Table 1). The reason for this discrepancy is that we use OGLE-IV collection of T2CEPs and ACEPs, while Groenewegen and Jurkovic (2017b) used data from the OGLE-III phase which covered significantly smaller area in the Magellanic System, *i.e.*, did not include the LMC northern spiral arm. Therefore, this is the first time we present PL relations based on the latest data.

In order to determine distances, we use the same method as Jacyszyn-Dobrzeniecka *et al.* (2016). However, we calculate distances separately for the LMC and SMC samples. Using appropriate PL relation and period P , we calculate reference Wesenheit magnitude W_{ref} (a and b coefficients from Table 1):

$$W_{\text{ref}} = a \cdot \log(P) + b. \quad (3)$$

In the next step we calculate the relative distance modulus:

$$\delta\mu = W_I - W_{\text{ref}}, \quad (4)$$

and the absolute distance given as:

$$d = d_{\text{LMC/SMC}} \cdot 10^{\frac{\delta\mu}{5}}, \quad (5)$$

where $d_{\text{LMC/SMC}}$ are the mean distances to the LMC (49.97 ± 1.11 kpc, Pietrzyński *et al.* 2013) and SMC (62.1 ± 1.9 kpc, Graczyk *et al.* 2014), respectively.

To perform statistical tests, we transform equatorial coordinates and distances (α, δ, d) to the three-dimensional Cartesian space (x, y, z) with equations given by van der Marel and Cioni (2001) and Weinberg and Nikolaev (2001):

$$\begin{aligned} x &= -d \cdot \cos(\delta) \sin(\alpha - \alpha_{\text{cen}}), \\ y &= d \cdot (\sin(\delta) \cos(\delta_{\text{cen}}) - \cos(\delta) \sin(\delta_{\text{cen}}) \cos(\alpha - \alpha_{\text{cen}})), \\ z &= d \cdot (\cos(\delta) \cos(\delta_{\text{cen}}) \cos(\alpha - \alpha_{\text{cen}}) + \sin(\delta) \sin(\delta_{\text{cen}})). \end{aligned} \quad (6)$$

This transformation assumes that the observer is in $(0, 0, 0)$ and the z axis is pointing toward the center of a Cloud at $(\alpha_{\text{cen}}, \delta_{\text{cen}})$. We transform LMC and SMC stars coordinates separately using the centers of the Magellanic Clouds based on the RR Lyr variables distributions (Jacyszyn-Dobrzniecka *et al.* 2017):

$$\begin{aligned} (\alpha_{\text{cen,LMC}}, \delta_{\text{cen,LMC}}) &= (5^{\text{h}}21^{\text{m}}31^{\text{s}}.2, -69^{\circ}36'36''), \\ (\alpha_{\text{cen,SMC}}, \delta_{\text{cen,SMC}}) &= (0^{\text{h}}55^{\text{m}}48^{\text{s}}.0, -72^{\circ}46'48''). \end{aligned} \quad (7)$$

To visualize and compare by eye stars distributions we use two-dimensional sky map in Hammer equal-area projection. We transform equatorial coordinates (α, δ) to coordinates in the Hammer system $(x_{\text{Hammer}}, y_{\text{Hammer}})$. In this coordinates transformation, the z axis is pointing toward $(\alpha_{\text{cen}}, \delta_{\text{cen}}) = (3^{\text{h}}20^{\text{m}}, -72^{\circ})$. Hammer coordinates are calculated as follow:

$$\begin{aligned} \alpha_{\text{b}} &= \alpha + \left(\frac{\pi}{2} - \alpha_{\text{cen}} \right), \\ l &= \arctan \left(\frac{\sin(\alpha_{\text{b}}) \cos(\delta_{\text{cen}}) + \tan(\delta) \sin(\delta_{\text{cen}})}{\cos(\alpha_{\text{b}})} \right) - \frac{1}{2}\pi, \\ \beta &= \arcsin(\sin(\delta) \cos(\delta_{\text{cen}}) - \cos(\delta) \sin(\delta_{\text{cen}}) \sin(\alpha_{\text{b}})), \\ x_{\text{Hammer}} &= -\frac{2\sqrt{2} \cos(\beta) \sin(\frac{l}{2})}{\sqrt{1 + \cos(\beta) \cos(\frac{l}{2})}}, \\ y_{\text{Hammer}} &= \frac{\sqrt{2} \sin(\beta)}{\sqrt{1 + \cos(\beta) \cos(\frac{l}{2})}}. \end{aligned} \quad (8)$$

Eqs.(6) and (8) are based on Eqs.(7–14) from Jacyszyn-Dobrzniecka (2016) though we applied a small correction to one of them (there was a typo in Eq.(8) and a coefficient of $-\frac{1}{2}\pi$ was missing in the right hand side). The correct version that we use here is presented above.

4. Method of Performing Statistical Tests

In order to compare three-dimensional distributions of pulsating stars from our collection we use the extended Kolmogorov-Smirnov (KS) statistical test. The two-sample two-dimensional version of the KS test was introduced by Peacock (1983), who found that this test is almost independent from the distribution type. This means that for large samples, critical values of the test statistics should not differ significantly. Gosset (1987) has extended the Peacock's idea to three-dimensional distributions. The test statistic D_n is defined as the maximum absolute difference between two cumulative distribution functions. In three-dimensional space, 8 pairs of cumulative distribution functions are needed to calculate the test statistic D_n . Peacock (1983) pointed out that it was better to work with the test statistic Z_n defined as follow:

$$Z_n = \sqrt{\frac{n_1 n_2}{n_1 + n_2}} D_n \quad (9)$$

where n_1 and n_2 are the sample sizes. Assuming that the first sample comes from the $F(x, y, z)$ distribution, and the second sample comes from the $G(x, y, z)$ distribution, we test the null (H_0) and alternative (H_1) hypotheses defined as follow:

$$H_0 : F(x, y, z) = G(x, y, z), \quad H_1 : F(x, y, z) \neq G(x, y, z) \quad (10)$$

where H_0 means that the analyzed samples come from the same distribution, while H_1 means that samples come from different distributions.

The Peacock's idea of the multidimensional, two-sample Kolmogorov-Smirnov test is implemented in the statistical software R (R Core Team – <https://www.R-project.org>). The package named `Peacock.test` (Xiao 2017 and <https://CRAN.R-project.org/package=Peacock.test>) allows calculating the test statistic D_n for two samples in two- and three-dimensional spaces. The test statistic D_n obtained in this calculation is converted to Z_n using the sample sizes n_1 and n_2 . Peacock (1983) determined that sizes of the tested samples n_1 and n_2 should be greater than 10, while Gosset (1987) indicated that the sample sizes must be greater than 5.

The main goal of this study is to examine similarities between spatial distributions of classical pulsators (DCEPs and RR Lyr variables) and T2CEPs or ACEPs. These similarities would allow us to better understand the nature of these stars, especially their possible evolutionary histories. We test all possible combinations of pairs of samples. Typically, the first sample with size n_1 contains T2CEPs or ACEPs, while the second sample with size n_2 consists of other classical pulsators. The groups of DCEPs or RR Lyr stars are much larger than other groups of pulsating stars. Therefore, we draw without returning a set of stars from classical pulsator distributions with size n_2 , which is three times larger than n_1 . We draw 1000 such samples, for which we compute the test statistics D_n , and later we convert it to Z_n . The statistical test for large samples requires a large amount of computational time, so we decided to count the tests repeatedly for smaller samples.

In their papers, Peacock (1983) and Gosset (1987) give empirical formulae for estimating probability p and testing the hypotheses. In the main part of our analysis, we use two-sided critical values of the “theoretical” test statistic Z_n for testing hypotheses and making decision whether to reject or accept H_0 . However, we compare our decision-making method with asymptotic equations given by Gosset (1987). We discuss a comparison of these two methods in Section 6.

To test our hypotheses, we have to use the “theoretical” distribution of the test statistic in order to be able to compare this distribution (and its critical values) to the distribution of the test statistic of the tested samples. Bearing in mind the distribution-independent property of this test, we decide to use different “theoretical” distribution for each tested pair of samples. The sizes of the tested samples are not so large, therefore, the critical values of the test statistics are slightly different in each cases. Taking advantage of the fact that our collection of pulsating stars is very large, we decided to build a “theoretical” distributions of the test statistics based on all DCEPs and RR Lyr stars. For example, to test the hypotheses for BL Her ($n_1 = 79$) and RR Lyr variables ($n_2 = 3n_1 = 237$), we need “theoretical” distribution based only on RR Lyr stars. Hence, we use RR Lyr stars distribution to draw without returning samples with sizes n_1 and n_2 , which were tested 5000 times. We assume to test the hypotheses at the significance level of $\alpha = 0.05$. Therefore, for each “theoretical” distribution of Z_n we calculate 2.5th and 97.5th percentiles. The regions with Z_n smaller or equal than 2.5th percentile and larger or equal than 97.5th percentile are the critical region of the test statistic (region of the H_0 rejection).

In the next step, we compare each Z_n calculated for our pulsating stars with critical values of the “theoretical” test statistic distribution. If the value of Z_n is in the critical region of the test statistic we conclude, that there are clear grounds to reject the null hypothesis H_0 , so we have to accept alternative hypothesis H_1 . However, when value Z_n is between 2.5th and 97.5th percentiles we can conclude, that there is no sufficient evidence to reject the null hypothesis H_0 , so we accept H_0 (hence, we called this region acceptability region). We assumed that there is no evidence to reject H_0 (and to indicate the possible similarity between two distributions) if at least 90% of the Z_n are in the region between critical values of the test statistics. Hence, we think that if over 900 test statistics are outside the rejection area, it is likely that we will be able to find similarity in the spatial distributions of stars.

In the current framework of stellar pulsations and evolution theories, the spatial distributions of classical pulsators should not depend on the pulsation mode, and so in our statistical tests we did not divide DCEPs, RR Lyr stars and ACEPs into smaller groups with distinct pulsation modes. Looking at the sky distributions of classical pulsating stars, the differences between F-mode and IO distributions are noticeable. However, our investigation shows that these differences are relatively small and they do not affect results of statistical tests. For instance, while testing

BL Her stars with RR Lyr variables, the percentage of the test statistics in the acceptability region is 91.80% when RRab and RRc stars are treated as one group, but in case of testing BL Her stars with RRab and RRc stars separately, there is 92.50% and 93.00% of Z_n in the acceptability region, respectively. We obtained very similar results for the tests W Vir stars with DCEPs. The percentage of the test statistics outside the critical region of the test is 97.10% when F-mode and 10 DCEPs are treated as a single group, and 93.90% and 90.70% when they are treated separately. These differences are very similar for the SMC stars. In the case of remaining pairs, the null hypothesis is rejected because it does not meet our acceptability criterion.

5. Results of our Analysis

In Tables 2 and 3, we present the results of our statistical tests for all tested pairs of samples in the LMC and SMC. Pairs of pulsating classes for which we can conclude similarity in their spatial distributions are marked in bold. All distributions of the test statistic Z_n in comparison to the “theoretical” distributions of the test statistic of the RR Lyr stars and DCEPs are presented in Fig. 4 for the LMC (two left panels) and for the SMC (two right panels). Using solid lines, we marked from the left 2.5th, 50th (median), and 97.5th percentiles. The areas marked in gray are the rejection areas of the null hypothesis H_0 .

In Figs. 5–7, we present spatial distributions of T2CEPs and ACEPs in comparison to the DCEPs and RR Lyr variables distributions. We present the most interesting cases only for which results are similar in both Magellanic Clouds. In Figs. 5–7, the top plot presents two-dimensional distributions of pulsating stars in the Magellanic Clouds in the equal-area Hammer projection (the coordinates transformation described in Section 3). The middle and the bottom plots present xy (face-on view), xz (plan view) and yz (edge-on view) planes for the LMC and the SMC, respectively. To estimate shapes of the galaxies in each projection we use a standard kernel density estimation (KDE) based on the DCEPs or RR Lyr stars. The densest areas are marked in navy blue. Additionally, in each projection we plot the normalized density contours.

The numbers of T2CEPs in the SMC are significantly smaller than in the LMC, therefore fitted PL relations have larger uncertainties (see Table 1). Taking it into consideration, our tests may not be very accurate (despite the lower limit on the samples sizes, Peacock 1983, Gosset 1987, which is 10, and 5, respectively). Due to these reasons, we think that our analysis should be based mainly on the LMC, while SMC should be treated as an additional clue, not the foundation to drawing conclusions.

5.1. BL Her

Statistical tests in the LMC indicate that the spatial distribution of BL Her and RR Lyr stars are similar (Fig. 4b, LMC). There is 91.80% of the test statistics in the

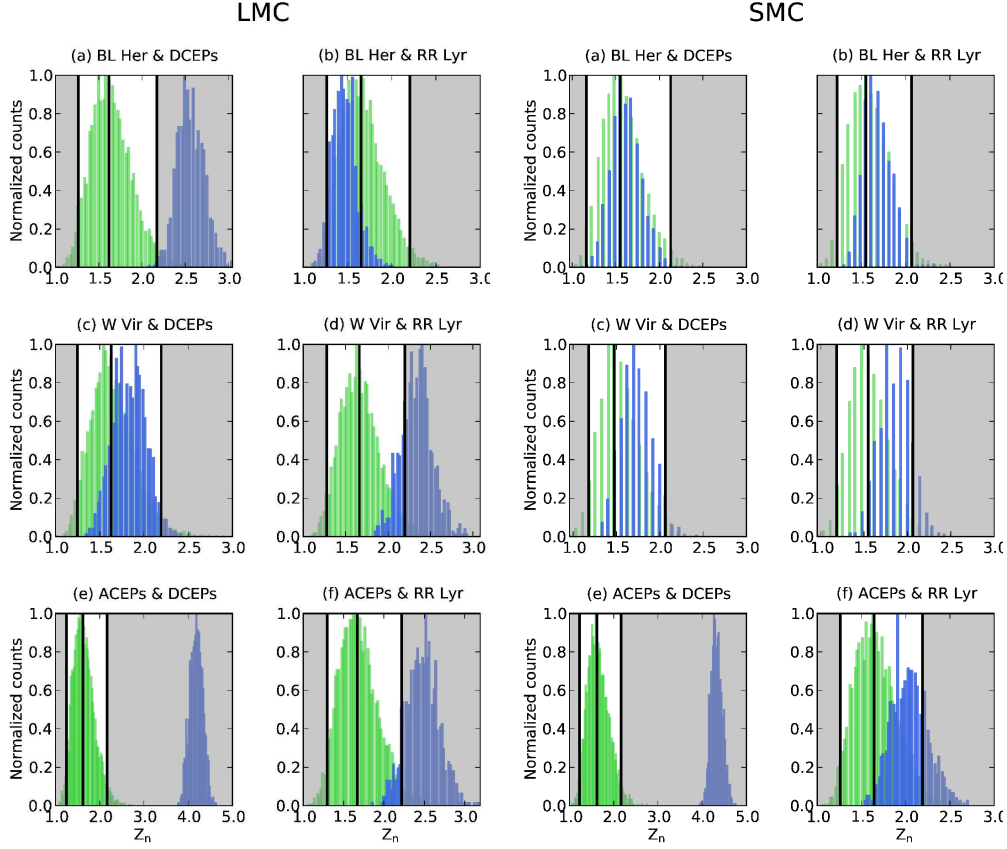


Fig. 4. Distributions of the test statistic Z_n for each tested pair of samples from the LMC (*two left panels*) and SMC (*two right panels*). With green color we marked “theoretical” distributions of the test statistic built based on DCEPs and RR Lyr stars, while blue histograms show the test statistic obtained during the tests of spatial distributions of T2CEPs and ACEPs with other classical pulsators. With solid, black lines we marked percentiles 2.5th, 50th (median), and 97.5th (from left side, respectively). The area marked in gray is the null hypothesis rejection area (critical region of the test statistic). Each plot represents different pair of tested samples.

acceptability region. This result is not surprising, because we expect that BL Her stars are old and have ages similar to the RR Lyr variables. Moreover, masses of the BL Her and RR Lyr stars are comparable (Groenewegen and Jurkovic 2017ab). In Fig. 5, we can see that some BL Her stars in the LMC are concentrated in the center of the galaxy, but the vast majority of these objects are distributed out of the center creating a vast halo, which is typical for old populations. In the SMC, the statistical tests for BL Her stars with RR Lyr variables give a comparable result (Fig. 4b, SMC). However, the difference is in the tests with DCEPs, for which we conclude similarities (Fig. 4a, SMC). As we mentioned before, it seems that this is due to a small number of T2CEPs in the SMC. Moreover, it is difficult to compare by eye these two distributions in the SMC with such small number of BL Her variables.

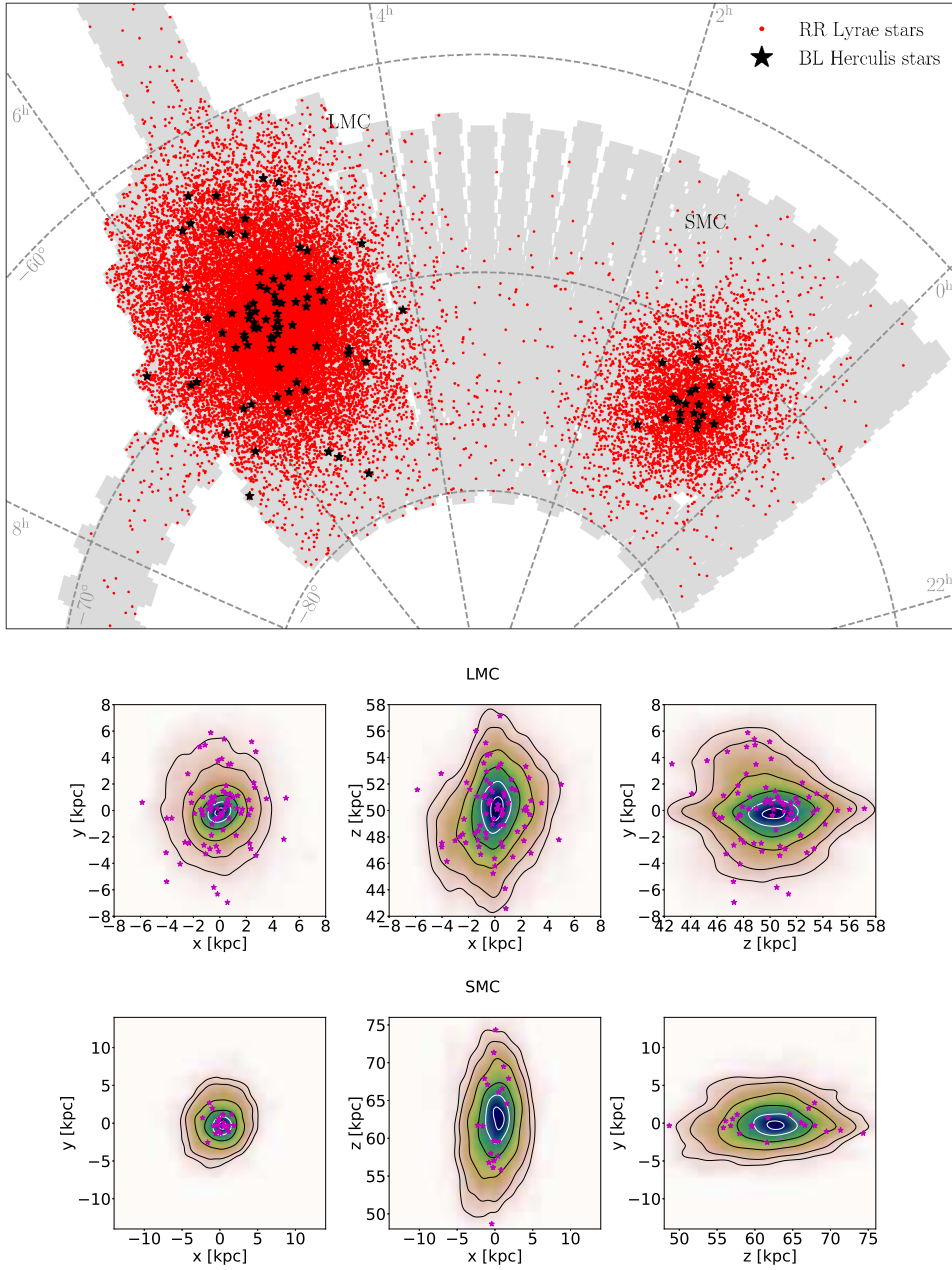


Fig. 5. Spatial distribution of BL Her stars in comparison to the distribution of RR Lyr stars. *Top panel* presents equal-area Hammer projection of the Magellanic System. Area marked in gray is the OGLE-IV footprint. *Middle and bottom panels* present Cartesian projections for the LMC and the SMC, respectively. We estimate shapes of the galaxies in each projection using standard kernel density estimation (KDE) and RR Lyr stars, which are marked with color map. Additionally, in each projection we plot normalized density contours. From the center of the galaxies to the edge, we plot normalized density with value: 95% (first white contour), 75% (second white contour), 50%, 25%, 10% and 5%. With magenta points, we marked BL Her stars.

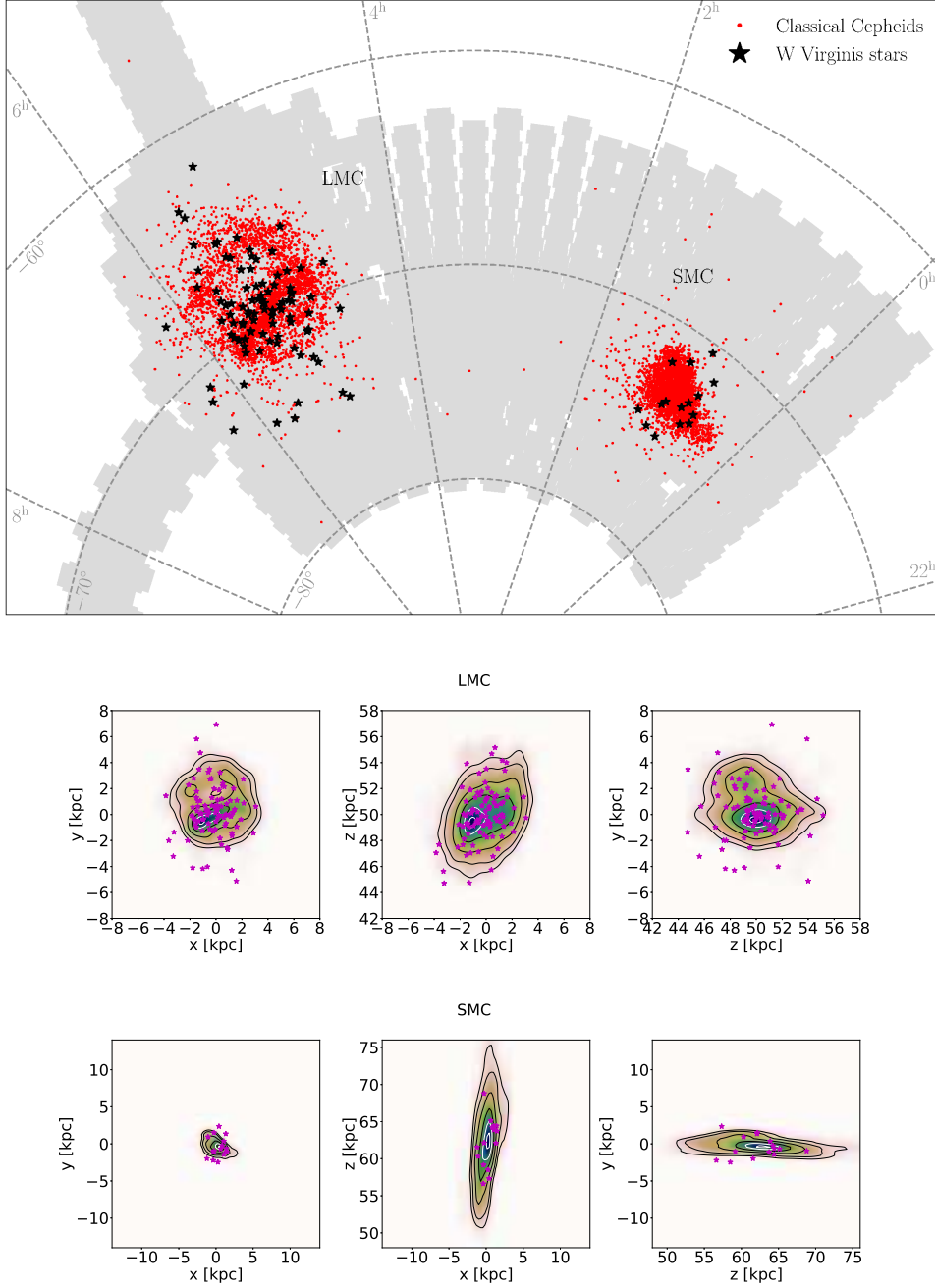


Fig. 6. Same as Fig. 5, but for W Vir stars and DCEPs.

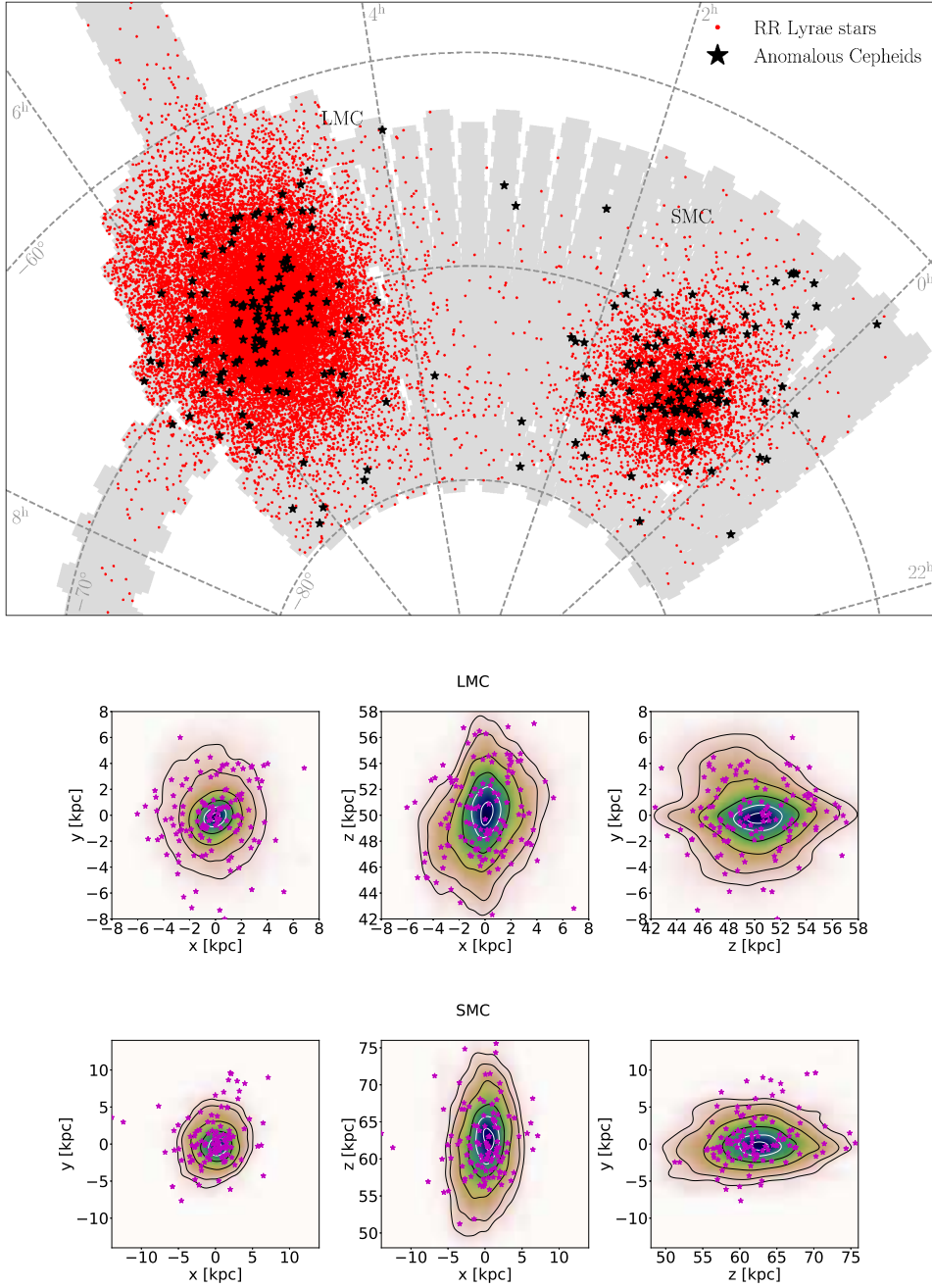


Fig. 7. Same as Fig. 5, but for ACEPs and RR Lyr stars.

Table 2

Results of the statistical tests in the Large Magellanic Cloud

tested samples (n_1 and n_2)	LMC							
	sample sizes		„theoretical” test statistics			test statistics of the tested samples		decision
	n_1	n_2	2.5th	50th	97.5th	% Z_n in crit. region	% Z_n in accept. region	
BL Her and DCEPs (Fig. 4a, LMC)	79	237	1.266	1.624	2.176	99.80	0.20	H_0 rejected
BL Her and RR Lyr stars (Fig. 4b, LMC)			1.267	1.656	2.209	8.20	91.80	H_0 accepted
W Vir and DCEPs (Fig. 4c, LMC)	94	282	1.251	1.638	2.203	2.90	97.10	H_0 accepted
W Vir and RR Lyr stars (Fig. 4d, LMC)			1.280	1.667	2.203	80.30	19.70	H_0 rejected
ACEPs and DCEPs (Fig. 4e, LMC)	133	399	1.252	1.627	2.178	100.00	0.00	H_0 rejected
ACEPs and RR Lyr stars (Fig. 4f, LMC)			1.301	1.677	2.228	92.50	7.50	H_0 rejected

Table 3

Results of the statistical tests in the Small Magellanic Cloud

tested samples (n_1 and n_2)	SMC							
	sample sizes		„theoretical” test statistics			test statistics of the tested samples		decision
	n_1	n_2	2.5th	50th	97.5th	% Z_n in crit. region	% Z_n in accept. region	
BL Her and DCEPs (Fig. 4a, SMC)	20	60	1.162	1.549	2.130	0.70	99.30	H_0 accepted
BL Her and RR Lyr stars (Fig. 4b, SMC)			1.226	1.549	2.066	3.10	96.90	H_0 accepted
W Vir and DCEPs (Fig. 4c, SMC)	15	45	1.193	1.491	2.087	5.50	94.50	H_0 accepted
W Vir and RR Lyr stars (Fig. 4d, SMC)			1.193	1.565	2.087	16.50	83.50	H_0 rejected
ACEPs and DCEPs (Fig. 4e, SMC)	111	333	1.233	1.617	2.165	100.00	0.00	H_0 rejected
ACEPs and RR Lyr stars (Fig. 4f, SMC)			1.260	1.644	2.192	25.90	74.10	H_0 rejected

Pairs of pulsating stars for which we can conclude similarity in their spatial distributions in Tables 2 and 3 are marked in bold

5.2. W Vir

Our statistical tests show that spatial distribution of W Vir stars is comparable to DCEPs in both Magellanic Clouds. The vast majority of the test statistics outside the rejection areas indicates that W Vir variables follow the distribution similar to that of young stars (Fig. 4c, LMC and SMC). The similarity of these two distributions is difficult to see in Fig. 6, taking into account the fact that some of these stars are located in the area where there is a halo which consists of the old stars, and where young stars are practically absent. In the tests of W Vir stars with RR Lyr variables in both Clouds (Fig. 4d, LMC and SMC), some of the test statistics are outside of the rejection area. In the LMC it is 19.70%, whereas in the SMC it is 83.50%. Therefore, the most important question is whether the similarity between W Vir stars and DCEPs is related to the structures created by young population stars, *i.e.*, the bar and spiral arms. The simplest test that can verify this thesis is to compare the spatial distribution of W Vir stars with RR Lyr variables, but with the limitation of the area in the three-dimensional space occupied by RR Lyr stars to the area occupied by DCEPs. We limit RR Lyr variables outskirts in the LMC to a sphere with a radius $R = 5$ kpc, where the vast majority of DCEPs are located. In Fig. 8 we present RR Lyr stars before and after limitation. Then, we compared W Vir stars distribution with the distribution of RR Lyr variables. In Fig. 9, we present “theoretical” distribution in comparison to the test statistic distribution for W Vir and RR Lyr stars. After RR Lyr halo cut, 94.80% of test statistics are out-

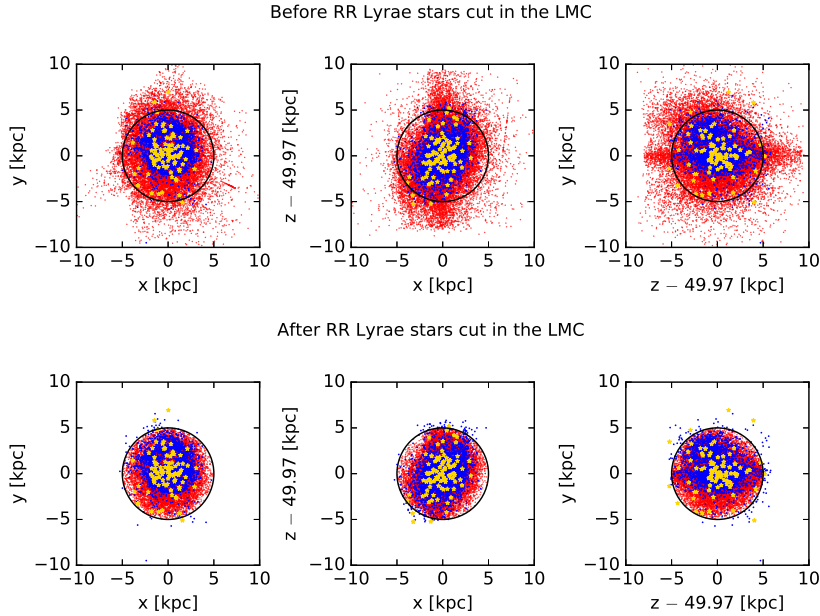


Fig. 8. Cutting procedure for RR Lyr outskirts regions in the Large Magellanic Cloud. With red dots we marked RR Lyr stars, blue dots correspond to DCEPs, while gold stars present W Vir distribution. Black circles represent the cut boundary of the RR Lyr stars halo, at the radius of $R = 5$ kpc.

side the rejection area. This result suggests that W Vir distribution similarities to DCEPs is not directly related to the structures created by the young population, but it is related to the lack of a big halo that RR Lyr stars form. Therefore, we are able to conclude that W Vir variables are intermediate-age stars with ages somewhere between DCEPs and RR Lyr variables, or they could be a mixture of an old and intermediate-age stars.

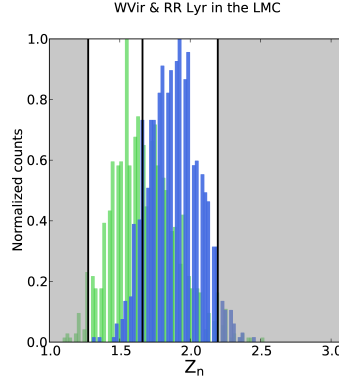


Fig. 9. Distribution of the test statistic Z_n for statistical test of W Vir stars with RR Lyr variables after the cut of outskirts regions in the LMC.

5.3. Anomalous Cepheids

The distribution of ACEPs in the Magellanic Clouds significantly differs from the distribution of DCEPs – all test statistics are in the rejection area of the null hypothesis (Fig. 4e, LMC and SMC). In the tests of ACEPs with RR Lyr stars (Fig. 4f, LMC and SMC), some of the test statistics are in the acceptability region. For the LMC, this value is 7.50%, whereas in the SMC it is 74.10%. Therefore, in the SMC this value is close to our acceptability criterion. Based on the statistical tests results, it is impossible to draw unambiguous conclusions. However, looking on the spatial distributions of ACEPs in comparison to RR Lyr stars distributions (Fig. 7), we can notice that ACEPs form a vast halo-like old population in the LMC, and even larger halo than RR Lyr variables in the SMC. Hence, it seems that ACEPs belong to the old population.

6. Comparison of the Decision Making Methods

Gosset (1987) provided asymptotic equations for estimating the probability p and making the decision about the hypotheses. These formulae are defined as follows:

$$1 - \frac{Z_n}{Z_\infty} = 0.75 \cdot \left(\frac{n_1 n_2}{n_1 + n_2} \right)^{-0.9}, \quad p \simeq 2 \exp(-3(Z_\infty - 1.05)^2). \quad (11)$$

By using them it is possible to calculate asymptotic value of test statistic Z_∞ for sample sizes n_1 and n_2 for which statistical test gives test statistic Z_n . We compared our results with the results obtained using the Gosset's equations. As before, we assumed a significance level $\alpha = 0.05$. It means, that if $p \leq 0.05$, we have to reject the null hypothesis, but if $p > 0.05$ there is no reason to reject the H_0 , so we accept it. For testing hypotheses using the Gosset's equations we decided to use significantly larger samples of classical pulsators. In general, we used all T2CEPs and ACEPs. Due to the very long computational time needed for calculation the test statistics for large samples in the three-dimensional space, we drew 20 times larger samples of stars from the LMC RR Lyr and DCEPs distributions. This means that we used 79 BL Her stars and 1580 DCEPs or RR Lyr variables, 94 W Vir stars and 1880 DCEPs or RR Lyr variables, and we tested 133 ACEPs with 2660 DCEPs or RR Lyr stars. In the SMC, we used the same number of DCEPs and RR Lyr variables in every case.

In the LMC, we have 100% agreement of both decision-making methods. In the SMC, one out of the six statistical tests gives a different result. There is a difference in the case of W Vir and RR Lyr stars test, where using the Gosset's equations the null hypothesis should be accepted. However, our result is very close to the acceptability criterion (the percentage of Z_n outside the rejection area is 83.50%). We find that the Gosset's equations do not work well in every case (*e.g.*, for tested pair BL Her stars with RR Lyr variables, probability p is greater than 1).

It should be noted that equations given by Gosset (1987) are only asymptotic approximations, therefore it is much better to rely on the critical values of the test statistic generated for the specific case. However, for simplified cases it is enough to use the equations given by Gosset (1987). A single different result out of all 12 tests means that the methods compatibility is at a 92% level.

7. Conclusions

In this work, we compared three-dimensional distributions of various classical pulsators. We used the OGLE collection of DCEPs, T2CEPs, ACEPs and RR Lyr stars (Soszyński *et al.* 2015a,b, 2016, 2017, 2018), and PL relations which we separately fitted to each group of pulsating stars. To compare the spatial distributions, we used the extended Kolmogorov-Smirnov test (Peacock 1983, Gosset 1987, Xiao 2017, <https://CRAN.R-project.org/package=Peacock.test>). As a main decision-making method, we used mock "theoretical" distributions based on all DCEPs and RR Lyr stars, for which we counted critical values of the test statistics. We compared our method with the asymptotic formulae given by Gosset (1987). We omitted peculiar W Vir and RV Tau stars in the analysis, because the distances to them were determined with large uncertainty.

Our results show that BL Her stars have a similar spatial distribution to that of RR Lyr variables. They clearly form an extended halo similar to the old population,

providing the evidence that BL Her stars are likely old. Moreover, four of BL Her stars from our sample are probable members of the LMC globular clusters that are known to be old (Soszyński *et al.* 2018). The masses of these variables are slightly smaller than those of RR Lyr stars (Groenewegen and Jurkovic 2017b). Additionally, modern evolutionary scenarios successfully reproduce the evolution of these stars. All the above conclusions allow us to infer, that BL Her stars have an age comparable to RR Lyr variables.

The comparison of the spatial distribution of W Vir stars to DCEPs and RR Lyr stars (also with halo cut, which is described in Section 5) suggests that the former variables are intermediate-age stars with age somewhere between DCEPs and RR Lyr stars. However, we found that one W Vir variable is a probable member of the LMC old globular cluster (Soszyński *et al.* 2018). For this reason, we are more inclined to conclude that these variables are a mixture of old and intermediate-age stars. An additional argument for this can be the masses of W Vir stars – they are comparable to BL Her stars masses (Groenewegen and Jurkovic 2017b). Moreover, following this we can also state that they are comparable to RR Lyr stars masses.

In the classical scenario of the T2CEPs evolution proposed by Gingold (1976, 1985), BL Her and W Vir variables should follow exactly the same spatial distributions, because both groups belong to the same stellar population. Our research shows, that distributions of considered T2CEPs subgroups are not exactly the same, which questions the Gingold’s scenario. The other piece of evidence is that blue loops through the instability strip are not reproduced in modern evolutionary calculations. This implies that we need other ideas about evolution of W Vir stars, which can be confirmed observationally.

Previous studies of the spatial distribution of ACEPs show that it is different than distributions of DCEPs or RR Lyr (Fiorentino and Monelli, 2012). Our results also do not provide unambiguous conclusions and are consistent with the previous ones. For ACEPs in the Magellanic Clouds, we can conclude with great certainty that three-dimensional distribution of these stars is completely different than the distribution of DCEPs. The statistical tests of the spatial distribution of these stars with RR Lyr variables do not give clear conclusions, because only in the SMC the majority of the test statistics are outside the rejection area. However, looking at the results from the SMC and having in mind the vast halo of ACEPs in both Clouds, we are inclined to the theory, that these stars belong to the old population. Their ages similar to the RR Lyr variables suggest that the most favorable evolution scenario for these stars is coalescence of two low-mass stars in a binary system. If these stars evolved as a single one, they should be definitely younger.

The similarities of the three-dimensional distributions of T2CEPs and ACEPs to the other classical pulsator distributions provide us with clues about the origin of these stars and their properties. However, our research is based on a statistical method, which by design requires numerous assumptions. In the SMC, differences in the distributions of the pulsating stars, compared with the LMC, are visible by

the naked eye (*e.g.*, the lack of spiral arms and bar in the DCEPs distribution). Therefore, we do not expect that the agreement for both Magellanic Clouds will be at 100%. Due to a greater number of such stars in the LMC, future analyses will be more statistically meaningful than the ones for the SMC.

Acknowledgements. We are grateful to the anonymous referee for suggestions and comments that greatly improved this publication. We would like to thank M. Marconi and M. Groenewegen for a fruitful discussion and valuable comments during 4th MIAPP programme 2018 “The Extragalactic Distance Scale in the Gaia Era” which took place from June 11 to July 6, 2018, in Garching, Germany. We also thank J.A. Peacock and Y. Xiao for advice regarding the idea of an multidimensional Kolmogorov-Smirnov test and its implementation in the R software.

This work has been supported by the National Science Centre, Poland, grant MAESTRO no. 2016/22/A/ST9/00009 to I. Soszyński. P. Iwanek is partially supported by the Kartezjusz programme no. POWR.03.02.00-00-I001/16-00 founded by The National Centre for Research and Development, Poland. The OGLE project has received funding from the National Science Center, Poland, grant MAESTRO no. 2014/14/A/ST9/00121 to A. Udalski.

REFERENCES

- Baade, W. 1952, *Trans. I.A.U.*, **8**, 397.
 Bono, G., Caputo F., Fiorentino, G., Marconi, M., and Musella, I. 2008, *ApJ*, **684**, 102.
 Braga, V.F., *et al.* 2015, *ApJ*, **799**, 165.
 Caputo, F., Marconi, M., Musella I., and Santolamazza, P. 2000, *A&A*, **359**, 1059.
 Cassisi, S., and Salaris M. 2013, in: “Old Stellar Populations: How to Study the Fossil Record of Galaxy Formation”, Wiley-VCH.
 Catelan, M., Pritzl, B.J., and Smith, H.A. 2004, *ApJS*, **154**, 633.
 Deb, S., Ngeow C.-C., Kanbur S.M., Singh H.P., Wysocki, D., and Kumar S. 2018, *MNRAS*, **478**, 2526.
 Dziembowski, W.A. 2016, *Communications of the Konkoly Observatory Hungary*, **105**, 23.
 Fiorentino, G., and Monelli, M. 2012, *A&A*, **540**, A102.
 Freedman, W.L., and Madore, B.F. 2011, *ApJ*, **734**, 46.
 Gieren, W., *et al.* 2018, arXiv 1809.04073.
 Gingold, R.A. 1976, *ApJ*, **204**, 116.
 Gingold, R.A. 1985, *Societa Astronomica Italiana, Memorie*, **56**, 169.
 Gosset, E. 1987, *A&A*, **188**, 258.
 Graczyk, D., *et al.* 2014, *ApJ*, **780**, 59.
 Groenewegen, M.A.T., and Jurkovic, M.I. 2017a, *A&A*, **603**, A70.
 Groenewegen, M.A.T., and Jurkovic, M.I. 2017b, *A&A*, **604**, A29.
 Inno, L., *et al.* 2016, *ApJ*, **832**, 176.
 Jaczyn-Dobrzeniecka, A.M., *et al.* 2016, *Acta Astron.*, **66**, 149.
 Jaczyn-Dobrzeniecka, A.M., *et al.* 2017, *Acta Astron.*, **67**, 1.
 Leavitt, H.S., and Pickering, E.C. 1912, *Harvard College Observatory Circular*, **173**, 1.
 Madore, B.F. 1976, in: “The Galaxy and the Local Group”, p. 153.
 Matsunaga, N., Feast, M.W., and Menzies, J.W. 2009, *MNRAS*, **397**, 933.
 Moskalik, P., *et al.* 2015, *MNRAS*, **447**, 2348.

- Netzel, H., Smolec, R., and Moskalik, P. 2015, *MNRAS*, **453**, 2022.
- Netzel, H., Smolec, R., Soszyński, I., and Udalski, A. 2018, *MNRAS*, **480**, 1229.
- Nikolaev, S., Drake, A.J., Keller, S.C., Cook, K.H., Dalal, N., Griest, K., Welch, D.L., and Kanbur, S.M. 2004, *ApJ*, **601**, 260.
- Peacock, J.A. 1983, *MNRAS*, **202**, 615.
- Pietrzyński, G., *et al.* 2013, *Nature*, **495**, 76.
- Prudil, Z., and Skarka, M. 2017, *MNRAS*, **466**, 2602.
- Prudil, Z., Smolec, R., Skarka, M., and Netzel, H. 2017, *MNRAS*, **465**, 4074.
- Romaniello, M., *et al.* 2008, *A&A*, **488**, 731.
- Schlegel, D.J., Finkbeiner, D.P., and Davis, M. 1998, *ApJ*, **500**, 525.
- Skowron, D.M., *et al.* 2016, *Acta Astron.*, **66**, 269.
- Smolec, R., and Śniegowska, M. 2016, *MNRAS*, **458**, 3561.
- Smolec, R., Prudil, Z., Skarka, M., and Bakowska, K. 2016, *MNRAS*, **461**, 2934.
- Soszyński, I., *et al.* 2008, *Acta Astron.*, **58**, 293.
- Soszyński, I., *et al.* 2015a, *Acta Astron.*, **65**, 233.
- Soszyński, I., *et al.* 2015b, *Acta Astron.*, **65**, 297.
- Soszyński, I., *et al.* 2015c, *Acta Astron.*, **65**, 329.
- Soszyński, I., *et al.* 2016, *Acta Astron.*, **66**, 131.
- Soszyński, I., *et al.* 2017, *Acta Astron.*, **67**, 103.
- Soszyński, I., *et al.* 2018, *Acta Astron.*, **68**, 89.
- Süveges, M., and Anderson, R.I. 2018, *MNRAS*, **478**, 1425.
- Thackeray, A.D. 1950, *The Observatory*, **70**, 144.
- Udalski, A. 2003, *ApJ*, **590**, 284.
- Udalski, A., Szymański, M.K., and Szymański, G. 2015, *Acta Astron.*, **65**, 1.
- Weinberg, M.D., and Nikolaev, S. 2001, *ApJ*, **548**, 712.
- Welch, D.L. 2012, *Journal of the American Association of Variable Star Observers (JAAVSO)*, **40**, 492.
- Wielgórski, P., *et al.* 2017, *ApJ*, **842**, 116.
- Xiao, Y. 2017, *Comput. Stat. Data Anal.*, **105**, 53.
- Zinn, R., and Searle, L. 1976, *ApJ*, **209**, 734.
- van der Marel, R.P., and Cioni, M.-R.L. 2001, *AJ*, **122**, 1807.